Available online at www.sciencedirect.com

SCIENCE DIRECT®

Journal of the European Ceramic Society 24 (2004) 2465–2470

www.elsevier.com/locate/jeurceramsoc

Positive temperature coefficient of resistivity in $Pb(Fe_{1/2}Nb_{1/2})O_3$ ceramics

Sang-Bop Lee*, Seok-Hyun Yoon, Hwan Kim

School of Materials Science and Engineering, Seoul National University, Seoul 151-742, South Korea

Received 10 January 2003; accepted 6 August 2003

Abstract

The positive temperature coefficient of resistivity (PTCR) effect in ferroelectric $Pb(Fe_{1/2}Nb_{1/2})O_3$ (PFN) ceramics was examined to determine its physical meaning as the evidence of the ferroelectric domain structure. Monitoring of the temperature dependence of resistivity showed that its PTCR effect begins around the dielectric maximum temperature (T_m). The existence of the space charge region near the grain boundary was verified via impedance spectroscopy, and X-ray photoelectron spectroscopy (XPS) indicated it to be due to Pb volatilization during the sintering process. In addition, well-development ferroelectric domain structure, which was expected to be found according to Jonker's theory, was observed with transmission electron microscopy (TEM).

Keywords: Domains; Lead iron niobate; $Pb(FeNb)O_3$; PTCR; TEM; XPS

1. Introduction

$Pb(Fe_{1/2}Nb_{1/2})O_3$ (PFN), a lead-based complex perovskite, is regarded as a good candidate as a multilayer ceramic capacitor owing to its high dielectric constant and low sintering temperature.[1–3] In addition, its intermediate position between normal ferroelectric (e.g.: $BaTiO_3$, $SrTiO_3$, etc) and relaxor ferroelectric (e.g.: $Pb(Mg_{1/3}Nb_{2/3})O_3$, $Pb(In_{1/2}Nb_{1/2})O_3$, etc.) materials has been suggested as the key to solve the secret of relaxor mechanism.[4,5]

The positive temperature coefficient of resistivity (PTCR) effect has been regarded as a good measure for identifying normal ferroelectric materials due to its relationship with the existence of ferroelectric macrodomains.[6,7] Since $BaTiO_3$ doped with small amount of donor impurities such as Y, Sb, La and Nb, $BaTiO_3$ has been reported to exhibit the PTCR behavior,[8–10] some lead-based perovskites with normal ferroelectric properties have also been found to exhibit this behavior.[11–13]

This effect has been reported to be attributed to the intergranular potential barrier from the surface charge capturing electrons. This barrier increases the room temperature resistivity, while it is lowered by the charge compensation effect of the ferroelectric domains. However, the resistivity begins to increase till all acceptor states are occupied over the Curie temperature (T_c) where the ferroelectric domains disappear and their charge compensation effect vanishes.[14] This conventional theory suggests two important necessary conditions for the occurrence of the PTCR effect; the intergranular potential barrier and the ferroelectric domain.

The fact that undoped PFN exhibits PTCR behavior is not expected in view of the conventional PTCR theory based on doped $BaTiO_3$, and it have not been properly explained. In this study the reason why undoped PFN shows this behavior was investigated. Furthermore, based on the fact that the ferroelectric domain structure is a necessary condition of the PTCR behavior, the ferroelectric domain structure in PFN was observed in order to identify its location between normal and relaxor ferroelectrics.

2. Experimental

2.1. Sample preparation and characterization

Reagent grade PbO (99.9%, High Purity Chem. Co., Japan), Nb_2O_5 (99.9%, High Purity Chem. co., Japan)

---

* Corresponding author. Tel.: +82-28807165; fax: +82-28841413.
E-mail address: palewind@plaza1.snu.ac.kr (S.-B. Lee).

0955-2219/$ - see front matter © 2003 Elsevier Ltd. All rights reserved.
doi:10.1016/j.jeurceramsoc.2003.08.009

and Fe_2O_3 (99.9%, High Purity Chem. Co., Japan) were used to prepare the PFN specimen. In order to synthesize the $FeNbO_4$ phase, a stoichiometric mixture of Nb_2O_5 and Fe_2O_3 in a stoichiometric molar ratio was ball-milled in ethanol with zirconia balls for 24 h, and heat-treated at 1000 °C for 24 h. Subsequently, the stoichiometric PbO and $FeNbO_4$ mixture was calcined at 900 °C for 2 h in order to synthesize the PFN perovskite phase. The obtained PFN powder was granulated by adding aqueous 10 wt.% PVA (poly vinyl alcohol) and passed through a 100-mesh sieve. The powder was pressed into disc shaped pellets and sintered at 1050 (PFN1050) and 1150 °C (PFN1150) for 2 h at a heating rate of 300 °C/h. To prevent PbO volatilization, the pellets were embedded in the powder of the same composition in a Pt crucible, and placed in an alumina crucible again.

The crystal structure of the sintered body was analyzed using X-ray diffractometry (XRD, M18XHF, MacScience, Japan) using Cu Kα radiation, and the ferroelectric domain structure was observed using transmission electron microscopy (TEM, CM-20, Phillips, Holland). X-ray photoelectron spectroscopy (XPS, ESCA Phi-5600, Physical Elecronics, USA) was used to measure the oxidation state of the lead in specimen.

2.2. Measurement of electrical properties

In order to measure the dielectric properties and resistivity, the two opposite faces of the specimen were painted with a silver paste and fired at 650 °C for 30 min. The dielectric properties were measured using an impedence analyzer (HP-4192, Hewlett Packard, Japan), and the resistivity was measured with a pA meter (HP-4140B, Hewlett Packard, Japan). Complex impedence spectroscopy (SI-1260, Solartron, UK) was used to separate the contribution of the grains and grain boundaries to the total resistivity.

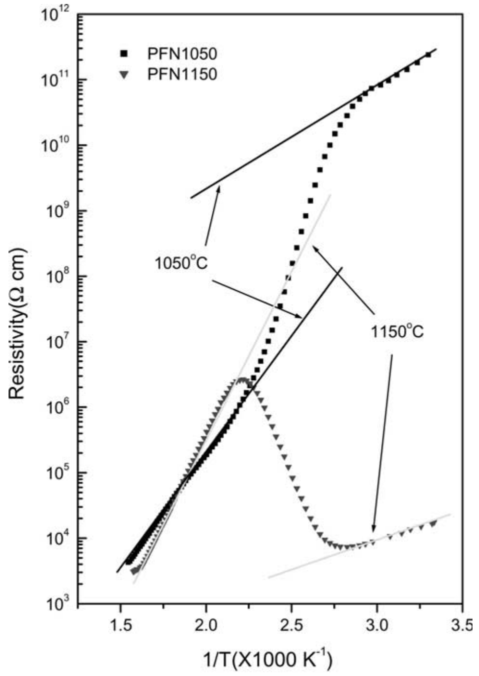

Fig. 2. Temperature dependence of the resistivity of PFN: (a) PFN1050 and (b) PFN1150.

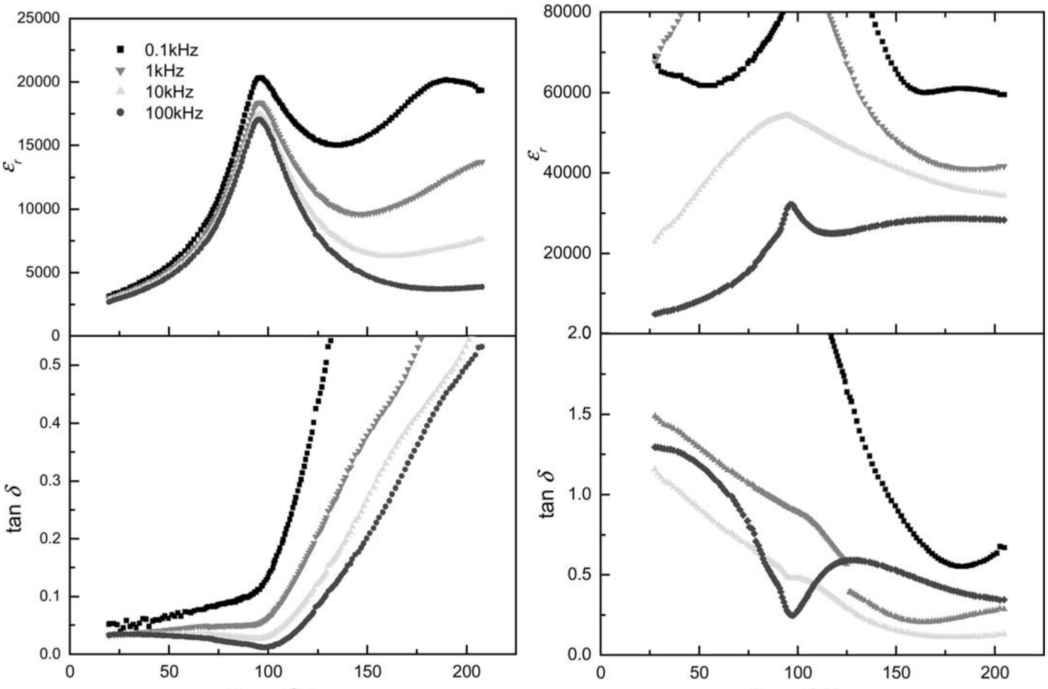

Fig. 1. Temperature dependence of the dielectric constant of PFN: (a) PFN1050 and (b) PFN1150.

3. Results and discussion

3.1. Structure and PTCR effect in PFN

XRD showed that the sintered body had a clean perovskite structure without any pyrochlore phase. The grain size of PFN1050 was 1–5 μm, and that of PFN1150 was 10–15 μm.

The temperature dependence of the dielectric constant (ϵ_r) and the dc resistivity (ρ) of PFN is shown in Figs. 1 and 2 respectively. In the case of PFN1150, DPT (diffuse phase transition) property was found, and the T_m (dielectrc maximum temperature) was 370 K and frequency-independent. The dielectric constant at T_m was 20,300 under a 100 Hz-frequency. A dielectric anomaly was shown, and the dielectric loss rapidly increased over the T_m. PFN1150 exhibited different dielectric properties compared to PFN1050, in that the graphs did not show a Gaussian relationship, and the dielectric loss over the whole temperature range was abnormally large, which was attributed to its low resistivity. In the case of PFN1050, the dc resistivity at room temperature was $\sim 10^{11}$ Ωcm, which decreased rapidly over T_m to $\sim 10^3$ Ω cm at 400 °C. However, an increase in the sintering

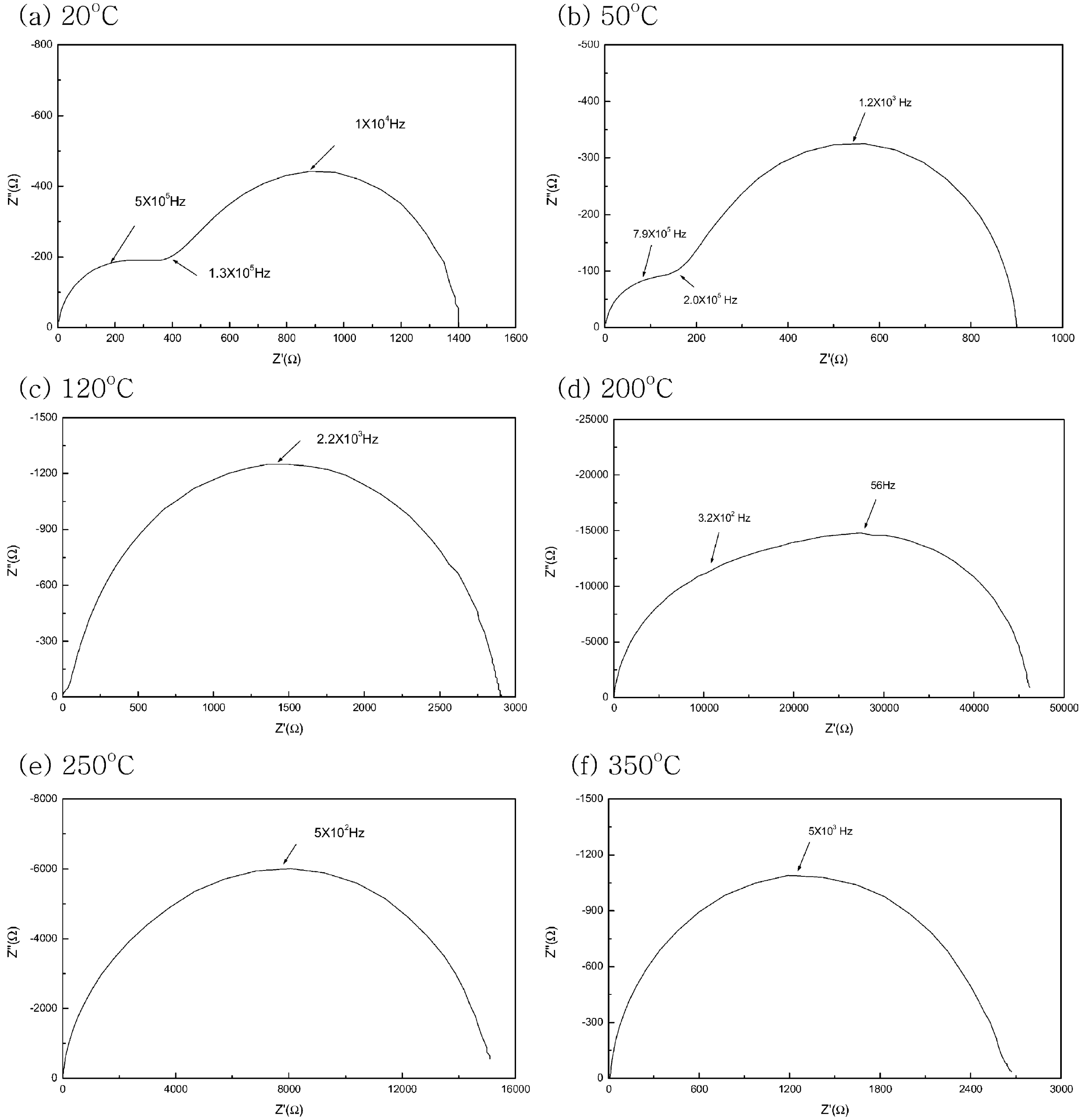

Fig. 3. Impedance spectroscopy of PFN1150.

temperature greatly decreased the dc resistivity of PFN at room temperature; $\sim 10^4\ \Omega$ cm in PFN1150. Its low resistivity is originated from the use of a very reducible element, Fe. The coexistence of Fe^{2+} and Fe^{3+} results in electron hopping between the two,[15–18] and we previously reported that the effect of the sintering temperature is attributed to the irreversible chemical change at the grain boundary.[19,20]

PFN1150 also showed the typical PTCR effect. Below T_m and over 250 °C, it showed a thermally activated conduction behavior, but the slopes were different. The resistivity can be obtained, in thermally activated conductionby the following equation:

$$\ln\rho = \ln\rho_0 + (E_\sigma/k_B)(1/T) \tag{1}$$

where ρ_0 is preexponential factor, E_σ the conduction activation energy, k_B the Boltzmann constant, and T the absolute temperature. Because the slope of resistivity is linearly dependent on E_σ, a change in the slope means that the conduction activation energy changed across the dielectric maximum temperature (T_m). The linearly fitted values of E_σ were 0.15 eV below T_m and 0.38 eV over 250 °C.

The complex impedance spectroscopy of PFN1150 is shown in Fig. 3. Two RC circuit elements of bulk and grain boundary were clearly shown at room temperature, but the resistivity increase of the grain boundary resulted in a superimposition of the two elements as temperature increased.

3.2. X-ray photoelectron spectroscopy

Nomura et al., who firstly reported the PTCR phenomenon in PFN, did not reveal any detailed mechanism for the unusual fact that undoped PFN had the space charge layer near the grain boundary while impurities form it in $BaTiO_3$.[21] The PTCR effect in the undoped Pb-containing compounds was analytically investigated using XPS by Nagamoto et al.[22] The results showed that the binding energy of $Pb4f_{7/2}$ was split into two energy states; one at 139 eV (peak A) and the other at 141 eV (peak B). Fig. 4 shows the spectra of the $Pb4f_{7/2}$ binding energy in PFN, which has a similar shape as the other lead-containing compounds with a PTCR effect.

It has been generally accepted that the split in the binding energy is attributed to the multivalency of lead (Pb^{2+} and Pb^{4+}), and Nagamoto et al. suggested that this multivalency cause the PTCR effect in $Ba_{1-x}SrP$-$SrPb_{1+y}O_3$.[22] Parmigiani approached the multivalency problem of lead by assuming two different electrical environments for the B cations due to the 1:1 chemical ordering in $Pb(Mg_{1/3}Nb_{2/3})O_3$. However, he could not prove a proper relationship between the multivalency and the chemical ordering.[23] Therefore, this hypothesis was alternated by the suggestion that lead had a formal valence of 2+, and peak A could be explained more reliably by a shift in the position of the lead cations from the normal lattice point in the randomly distributed region of B-site cations. He also suggested the possibility that lead and/or oxygen vacancies can control the charge neutrality in the ordered region. However, even this suggestion could not explain the phenomenon shown in Fig. 4 in that the relative intensity of peak A was affected by the extent of lead volatilization in PFN, which means that an increase in the [V_{Pb}''] was the determining factor for the relative intensity between peak A and B.[24] It would be more reasonable to say that Pb and/or oxygen vacancies affect the position shift of lead cations from the lattice point.

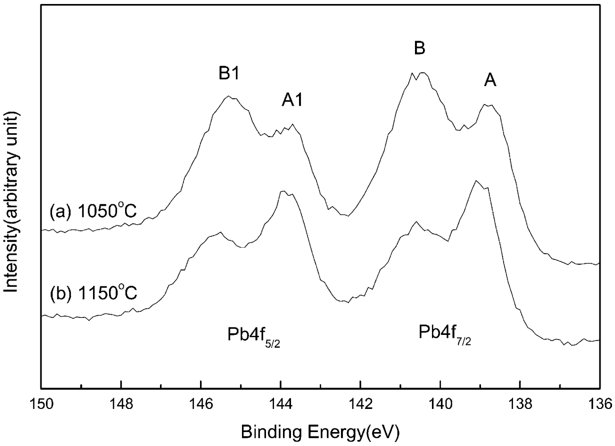

Fig. 4. Slow scan XPS spectra of the $Pb4f_{7/2}$ states of PFN: (a) PFN1050 and (b) PFN1150.

It was reported that a diffused layer of cation vacancies form the space charge layer near the grain boundary, and particularly the A-site cation (barium) is easier to diffuse than the B-site cation (titanium).[25,26] Lead vacancies generally diffuse from the grain boundary into the inner grain during sintering. Consequently a space charge layer in PFN is likely to be formed by the Pb volatilization during sintering. However, the resistivity did not increase, although the vacancy concentration increased. This is because the volatilization of Pb volatilization increased the relative Fe concentration at the grain boundary, which made electron hopping between the Fe sites easier.[19]

3.3. Ferroelectric domain structure in PFN

The PTCR effect in PFN implies the existence of ferroelectric domains, which provides good information on its ferroelectric properties, particularly its intermediate location between normal and relaxor ferroelectrics. According to Jonker's theory, resistance lowering below T_c can be attributed to the weakened potential barrier by the ferroelectric domains.[12,27]

The TEM photographs in Fig. 5 shows the domain structure and diffraction patterns in PFN1150. The

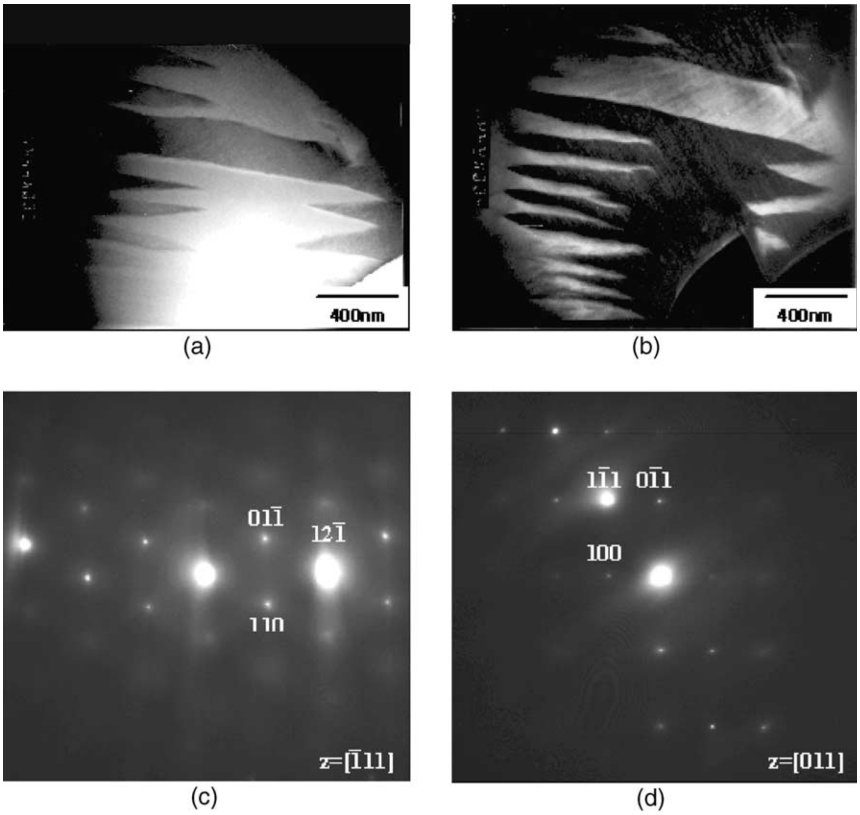

Fig. 5. TEM photographs and diffraction pattern of PFN1150, which show the ferroelectric domain structure: (a) dark field image, (b) bright field image, (c) diffraction pattern (zone axis = [$\bar{1}$11]) and (d) diffraction pattern (zone axis = [011]).

net area was divided into two regions with a clear black-and-white contrast, and each region had diagonal lines in it. The diffraction patterns with the [011] zone axis in Fig. 5(d) did not show any superlattice point [1/2 1/2 1/2], which means that the B-site cations are randomly disordered. Therefore we can conclude that the domain structure shown in Fig. 5 was attributed not to the ordering of B-site cation but to the ferroelectric dipole ordering.

Although Pb-containing relaxors have electric dipoles, ferroelectric macro-domains have not found in a TEM study except for ordered $Pb(Sc_{1/2}Ta_{1/2})O_3$ (PST), perovskite with titanium and poled-relaxors.[6,7] Furthermore, ordered PST is regarded as a normal ferroelectric material. Therefore, the existence of ferroelectric domains in PFN means that PFN is close to a normal ferroelectric material.

4. Conclusion

PFN1150 exhibited a PTCR Effect around the T_m, and the thermal activation energy over 250 °C was ~0.35 eV, while that below T_m was ~0.17 eV. Impedance spectroscopy showed the RC component from the space charge layer near the grain boundary, which is originated from the formation of Pb and O vacancies by Pb volatilization. The ferroelectric domain structure, which was expected from Jonker's theory, was observed by TEM.

Acknowledgements

This work was supported in part by the Korea Science and Engineering Foundation through the Ceramic Processing Research Center (CPRC) at Hanyang University.

References

1. Lee, B. H., Min, K. K. and Kim, N. K., Effect of PFT substitution on dielectric properties of PFW–PFN perovskite ceramics. *J. Mater. Sci.*, 2000, **35**, 197–201.
2. Jun, S. G. and Kim, N. K., Synthesis and dielectric properties of perovskite ceramic system $PFW_{0.8-x}\cdot PMN_{0.2}\cdot PFN_x$. *J. Mater. Sci.*, 2000, **35**, 1459–1463.
3. Ananta, S. and Thomas, N. W., Fabrication of PMN and PFN ceramics by a two-stage sintering technique. *J. Eur. Ceram. Soc.*, 1999, **19**, 2917–2930.
4. Cross, L. E., Relaxor ferroelectrics. *Ferroelectrics*, 1987, **76**, 241–267.
5. Randall, C. A., Bhalla, A. S., Shrout, T. R. and Cross, L. E., Classification and consequences of complex lead perovskite ferroelectrics with regard to B-site cation order. *J. Mater. Res.*, 1990, **5**, 829–834.
6. Randall, C. A., Barber, D. J. and Whatmore, R. W., In situ TEM

experiments on perovskite-structured ferroelectric relaxor materials. *J. Microscopy*, 1987, **145**, 275–291.

7. Lee, J. K., Yi, J. Y., Hong, K. S., Park, S. E. and Millan, J., Domain configuration and crystal structure of Pb($Zn_{1/3}Nb_{2/3}$)O_3-5%PbTiO_3 crystals as a function of the electric field direction. *J. Appl. Phys.*, 2002, **91**, 4474–4478.
8. Heywang, W., Bariumtitanat als Sperrschichthalbleiter. *Solid State Electronics*, 1961, **3**, 51–58.
9. Heywang, W., Resistivity anomaly in doped barium titanate. *J. Am. Ceram. Soc.*, 1964, **47**, 484–490.
10. Daniels, J. and Härdtl, K. H., Part I. Electrical conductivity at high temperatures of donor-doped barium titanate ceramics. *Philips Res. Repts.*, 1976, **31**, 489–504.
11. Kuwabara, M., Lead titanate ceramics with positive temperature coefficients of resistivity. *J. Am. Ceram. Soc.*, 1990, **73**(5), 1438–1439.
12. Lai, C. H., Lu, Y. Y. and Tseng, T. Y., Investigation of resistivity and permittivity for (Ba,Pb)TiO_3 PTCR ceramics. *J. Am. Ceram. Soc.*, 1994, **77**(9), 2419–2424.
13. Lin, Y. Y., Hu, C. T., Chang, H. Y. and Lin, I. N., Electrical properties of the positive temperature coefficient of resistivity materials with 490 °C critical temperature. *J. Appl. Phys.*, 1998, **83**(1), 1321–1326.
14. Jonker, G. H., Some aspects of semiconducting barium titanate. *Solid State Electronics*, 1964, **7**, 895–903.
15. Ichinose, N. and Kato, N., Dielectric properties of Pb($Fe_{1/2}Nb_{1/2}$)O_3 ferroelectric ceramics. *J. Mater. Sci. Lett.*, 1986, **15**, 864–866.
16. Wang, X., Gui, Z., Li, L. and Zhang, X., Mössbouer study on valency state of iron ions in Pb($Fe_{1/2}Nb_{1/2}$)O_3 ceramics. *Mater. Lett.*, 1994, **20**, 75–78.
17. Wang, X., Zhang, X. and Gu, B., Studies of Mössbauer spectrum on Pb($Fe_{1/2}Ta_{1/2}$)O_3 ferroelectric cermics. *J. Mater. Sci. Lett.*, 1996, **15**, 864–866.
18. Ananta, S. and Thomas, N. W., Relationships between sintering conditions, microstructure and dielectric properties of lead iron niobate. *J. Eur. Ceram. Soc.*, 1999, **19**, 1873–1881.
19. Lee, S. B., Lee, K. H. and Kim, H., The role of the grain boundary on the room temperature resistivity of Pb($Fe_{1/2}Nb_{1/2}$)O_3. *Jpn. J. Appl. Phys*, 2002, **41**, 5266–5271.
20. Lee, S. B., Lee, K. H. and Kim, H., The role of the grain boundary on the resistivity of Pb($Fe_{1/2}Nb_{1/2}$)O_3 at room temperature. *Mater. Res. Soc. Symp. Proceedings, Mater. Res. Soc.*, 2002, **718**, 207–212.
21. Nomura, S. and Doi, K., PTC effect in Pb$(FeNb)_{1/2}O_3$. *Jpn. J. Appl. Phys*, 1970, **9**, 716.
22. Nagamoto, H., Kagotani, H., Okubo, T. and Koya, T., Positive temperature coefficient of resistivity in $Ba_{1-x}Sr_xPb_{1+y}O_{3-\delta}$ ceramics. *J. Am. Ceram. Soc.*, 1993, **76**, 2053–2058.
23. Parmigiani, F., Rollandi, L., Samoggia, G. and Depero, L. E., X-ray photoelectron study of the relaxor lead magnesium niobate. *Solid State Comm.*, 1996, **100**, 801–805.
24. Lee, S. B., *A Study on Grain Boundary Resistivity and PTCR Properties of Pb($Fe_{1/2}Nb_{1/2}$)*O_3. PhD thesis, Seoul National University, Seoul, Korea, 2002.
25. Daniels, J., Härdtl, K. H. and Wernicke, R., The PTC effect of barium titanate. *Philips Tech. Rev.*, 1978, **38**, 73–82.
26. Lewis, G. V., Catlow, C. R. A. and Casselton, R. E. W., PTCR effect in $BaTiO_3$. *J. Am. Ceram. Soc.*, 1985, **68**, 555–558.
27. Jonker, G. H., Eulibrium barriers in PTC thermisters. In *Advanced in Ceramics, Vol. 1*, ed. L. M. Levinson. Am. Ceram. Soc, Columbus, OH, 1981, pp. 155–165.